

ELECTRON BEAM DYNAMICS IN THE ALICE IR-FEL FACILITY

F. Jackson, D. Angal-Kalinin, J. W. McKenzie, Y. M. Saveliev, T. Thakker, N. Thompson,
P. H. Williams, STFC Daresbury Laboratory, ASTeC & Cockcroft Institute, UK.
A. Wolski, University of Liverpool, UK.

Abstract

The ALICE facility at Daresbury Laboratory is an energy recovery test accelerator which includes an infra-red oscillator-type free electron laser (IR-FEL). The longitudinal phase space of the electron bunches and the longitudinal transport functions in the ALICE accelerator are studied in this paper.

INTRODUCTION

The ALICE (Accelerators and Lasers in Combined Experiments) facility is an energy recovery test accelerator [1][2] operated at Daresbury Laboratory since 2006 [3].

The accelerator consists of: a photoinjector with DC gun (up to 350 keV), buncher and superconducting booster (typically 6.5 MeV beam energy); a main energy-recovery loop (typically 26 MeV beam energy) containing a superconducting linac module, a bunch compression chicane, and an undulator.

ALICE is a test facility which has pursued several different goals and applications including an infra-red free-electron laser (IR-FEL) of the cavity oscillator type, and a terahertz (THz) research programme. In addition, ALICE serves as the injector to EMMA, the non-scaling FFAG (fixed field alternating gradient) demonstration machine [4]. Historically, the first application of ALICE was a demonstration of Compton backscattered x-rays [5].

The main demands on the ALICE beam dynamics and beam quality comes from the IR-FEL [6] which requires small energy spread (roughly 0.5%) and a small compressed bunch length (roughly 1 ps).

Throughout the operation of ALICE, beam delivery to the various applications has taken priority over fine measurement of beam dynamics or detailed machine characterisation. The machine design, especially beam transport and optics, has proved reasonably robust; pragmatic optimisation of machine performance has usually been sufficient for successful operation of the different applications. More recently, with greater reliability in application delivery, efforts to investigate the beam dynamics in a more systematic way have begun [7][8].

The first attempts to achieve IR-FEL operation were unsuccessful until the average beam current was reduced by reducing the bunch repetition frequency from its design value of 81.25 MHz, strongly implying beam loading effects causing energy droop over the bunch trains. The normal bunch repetition rate for the IR-FEL is currently 16.25 MHz.

The main beam dynamics factors relevant to the IR-FEL include the following: transverse steering and focussing of the beam in the FEL cavity; optimisation of the ALICE injector dynamics; and finally optimisation of the longitudinal beam transport in the main energy recovery loop including the arcs and bunch compressor.

The steering and focussing in the undulator is determined by intra-undulator beryllium alignment wedges which provide both optical alignment of the cavity mirrors and steering of the electron beam. The use of the wedges is usually sufficient to provide alignment of the electron beam with the undulator and oscillator cavity, and beam position monitors (BPMs) in the undulator section of the beamline are not usually required.

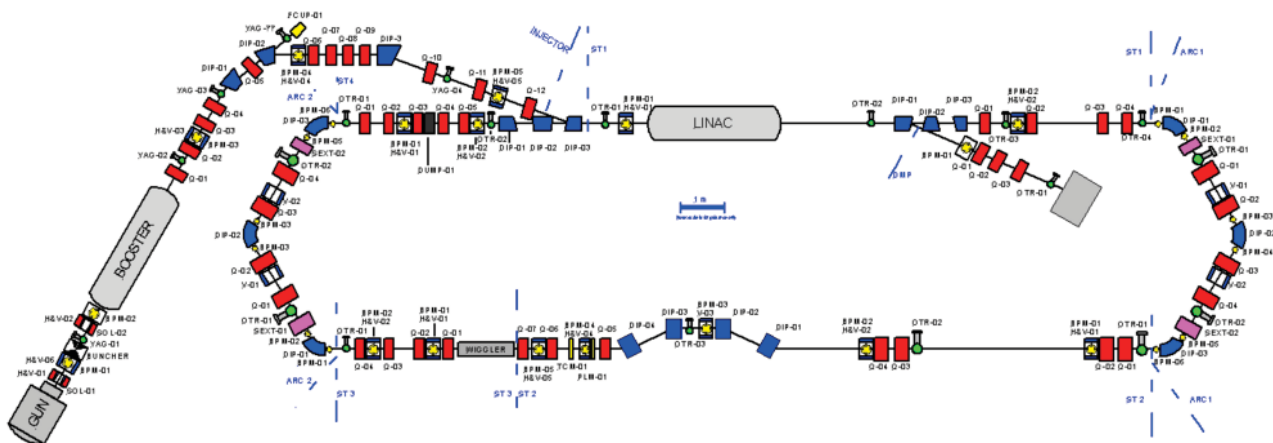


Figure 1: Layout of the ALICE accelerator.

The ALICE injector dynamics place strong constraints on the minimum energy spread and minimum compressed bunch length in the undulator. Due to the low energy of the beam in the injector space charge and velocity bunching or debunching effects may contribute significantly and are not fully understood or measured in detail with the current available diagnostics.

The longitudinal transport in the main loop is controlled by the properties of the arcs and bunch compressor. The bunch compressor is a simple four dipole chicane with fixed geometry and so its longitudinal transport properties are largely fixed with momentum compaction given by $|R_{56}| = 0.28$ m. The first arc has a flexible R_{56} and this flexibility is used frequently in pragmatic tuning of the post-linac dynamics to optimise FEL performance.

LONGITUDINAL PHASE SPACE MEASUREMENTS

Injector Measurements

As mentioned above, the injector longitudinal dynamics strongly influence the final bunch compression.

The minimum bunch length (and thus highest peak current) achievable at the FEL is determined by the intrinsic (i.e. uncorrelated) energy spread of the beam. The minimum bunch length is estimated by $\delta_0 \cdot R_{56} \cdot E_0 / E_m$ (see [7]), where δ_0 is the uncorrelated fractional energy spread at the entrance to the linac, R_{56} is the linac-to-undulator momentum compaction (magnitude of 0.28 m is the design value for ALICE), E_0 is the injector beam energy (typically 6.5 MeV) and E_m is the post-linac beam energy (typically 26 MeV). Thus, to achieve a minimum bunch length of 1 ps (0.30 mm) would require an uncorrelated energy spread of $\delta_0 = 0.5\%$ (30 keV) at the linac entrance.

The energy spread at the FEL is crucial for the FEL gain and is determined by the bunch length at the linac entrance. The energy spread as a function of the bunch length Δz is estimated by

$$\Delta E = \sqrt{\Delta E_0^2 + h^2 \Delta z^2} \quad (1)$$

where ΔE_0 is the uncorrelated energy spread and the chirp h is given by $E_L \frac{2\pi}{\lambda} \sin(\phi - \phi_0)$ where E_L is the on-crest linac energy gain (around 20 MeV), λ is the RF wavelength (231 mm), ϕ_0 is the linac phase at which the energy spread is minimised ($\phi_0 = 0$ if the bunch enters the linac with zero chirp), and ϕ is the off-crest phase. At the design off-crest phase of 10° , and for an typical intrinsic energy spread of 30 keV, an energy spread $\Delta E = 200$ keV at the FEL requires an injected bunch length of around $\Delta z = 2.0$ mm (7 ps).

Dedicated longitudinal phase space diagnostics have not been available on a routine basis at ALICE. Initially, bunch length measurements in the injector were performed in the gun and injector commissioning with a

transverse deflecting cavity [9], while energy spread was measured by screen images at dispersive locations. Coherent THz emission in the bunch compression chicane was initially used as a crude indication of bunch compression.

Later, methods of RF manipulation of the beam using the booster and main linac cavities were used to measure the bunch length in the injector and post linac, following the ‘‘zero phasing’’ procedure set out in [10]. However, the practical implementation of this method in ALICE has proved challenging. In the injector the beam dynamics and beamline characteristics result in very large bunch energy spreads at the RF zero phase points, much larger than can be measured directly using the dipole-to-screen spectrometer located there. The large energy spread can be measured by dipole scanning but the method is cumbersome. In addition the non-dispersive beams size is significant and is only minimised in the measurements in an ad-hoc fashion. Figure 2 shows the injector bunch length measured as a function of the phase of the first booster cavity, the trend indicating some agreement with simulation.

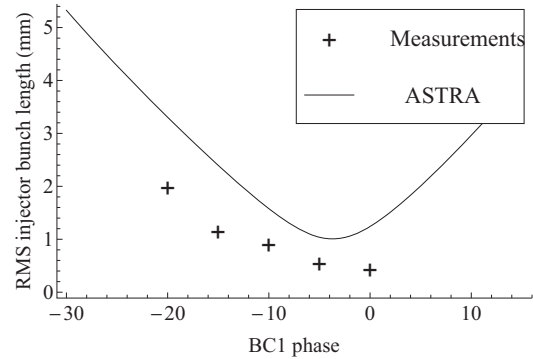


Figure 2: Injector bunch length measurement and simulation as a function of the first booster cavity (BC1) phase.

Over a large period of time the consistency of the injector bunch length measurements for ostensibly identical machine set-ups has shown limited consistency, see Figure 3.

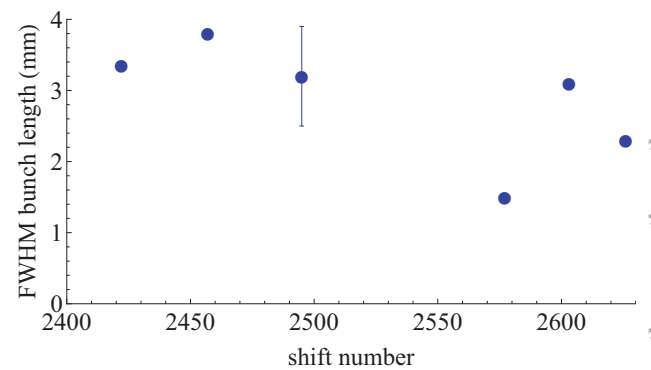


Figure 3: Injector bunch length measurements for a single machine set-up over a 5-month period. The measurement error was estimated on occasion and is indicated by the error bar.

Post-Linac Measurements

A non-disruptive electro-optic (EO) method of bunch length measurement has been utilised at ALICE to provide measurements of the compressed bunch[11]. The apparatus requires a dedicated femto-second laser to probe the coulomb field of the compressed bunch. The electro-optic method requires significant set-up and operational effort and thus its use has been limited to confirming the compression of bunches to the ps level; only limited studies have been performed of the sensitivity of the compressed bunch profile to different lattice conditions[8].

POST-LINAC LONGITUDINAL TRANSPORT

By design the ALICE lattice in the main loop consists of an isochronous first arc, a bunch compressor with $R_{56} = -0.28$ m, and a second arc with $R_{56} = +0.28$ m. The arc design is based on triple bend achromats (TBA) [12] and the R_{56} is tunable by the strengths of quadrupoles within the arc.

The R_{56} tunability of the first arc strongly influences the post linac bunch compression, as predicted in [12]. Sensitivity of the coherent THz emission from the chicane to the arc quadrupole strengths has been observed [7]. In addition these quadrupoles are frequently used when optimising the performance of the IR-FEL. The effect of the arc sextupoles is less clear, practical experience has indicated that the two sextupoles in the first arc have different effects on the THz emission.

To measure more quantitatively the longitudinal transport of the first arc and compression chicane, time of arrival measurements of the electron bunches were performed using BPMs at different locations. ALICE contains many stripline and button BPMs throughout the lattice. The timing of the raw BPM signals from the arriving electron bunches can be measured using a high resolution oscilloscope (40 giga samples per sec). Using a fixed reference signal from the ALICE master oscillator, the relative time of flight (or relative path length) of the bunches can be deduced. Varying the beam energy allows transport matrix elements R_{56} and T_{566} to be calculated from these measurements, using the approximation

$$\Delta z \approx R_{56}\delta + T_{566}\delta^2 \quad (2)$$

where z is the longitudinal coordinate and δ is the energy deviation with respect to the beam reference trajectory. The measured path length l is a relative quantity that can be modelled by $\Delta z + l_0 + C$, where l_0 is the reference trajectory path length and C is an arbitrary constant (depends on the reference signal used in the measurement). Fitting a parabolic curve to l vs. δ , the coefficients yield R_{56} and T_{566} . The feasibility of the experimental method was demonstrated in [8]; a time of flight resolution of approximately 1 ps is obtainable.

The relative path length was measured using button BPMs at the exit of the first arc and the exit of the

compression chicane, varying the beam energy by varying the main linac gradient.

The effect of the arc quadrupoles was studied in both locations. There are four quadrupoles in the first arc located symmetrically about the central dipole. The outer two quadrupoles (called “ar1q1” and “ar1q4”) have the greatest influence the R_{56} . Their effect on the relative path length at the arc exit and the compression chicane exit is seen in Figure 4 and Figure 5. The differences in the gross shapes of the l vs. δ curved between post-arc and post-chicane measurements is due to the larger R_{56} contribution post-chicane.

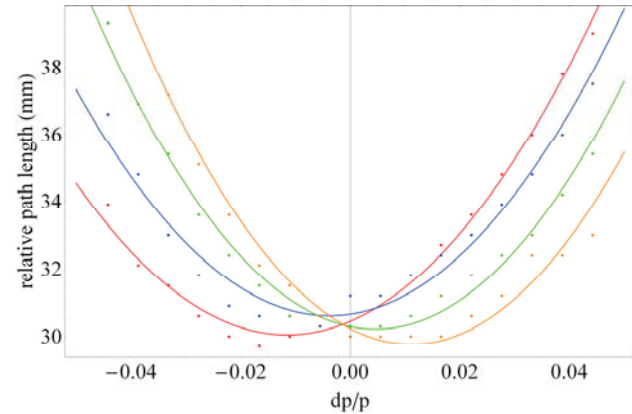


Figure 4: Relative path length vs beam energy measured at the exit of the first arc as the arc quadrupole strengths are varied. Points are measurements, lines are parabolic fits. Red, blue, green, orange colour sequence represents increasing quadrupole strength.

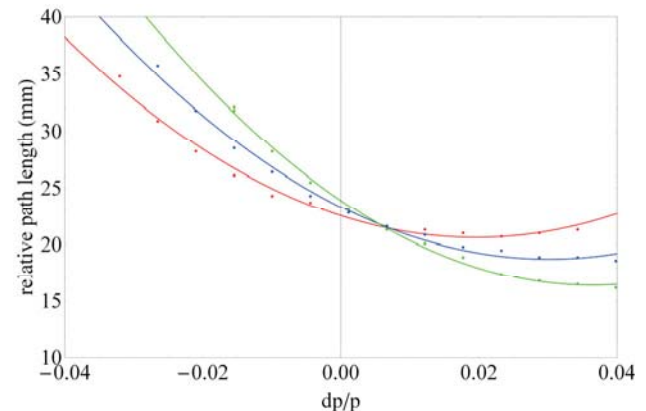


Figure 5: Relative path length vs. beam energy measured at the exit of bunch compressor as the arc quadrupole strengths are varied. Points are measurements, lines are parabolic fits. Red, blue, green, colour sequence represents increasing quadrupole strength.

The R_{56} of the lattice at the exit of the first arc and the bunch compressor can be extracted from the parabolic fits to the curves in Figure 4 and Figure 5, to measure the dependence of R_{56} on the first arc quadrupoles. The results are seen in Figure 6. These results indicate, as expected, a strong dependence of the R_{56} in the post-linac lattice on these quadrupoles and also indicate that the R_{56}

contribution of the compression chicane is around 0.30 m as expected.

The effect of the sextupoles in the first arc were measured and the results are displayed in Figure 7, clearly indicating modification of the path length curvature (T_{566}) by the sextupoles. The systematic difference observed between the effect of the two sextupoles is likely to be due to different misalignments of the beam with each sextupole. The misalignment results in a change in the lattice R_{56} as the sextupole strength is varied.

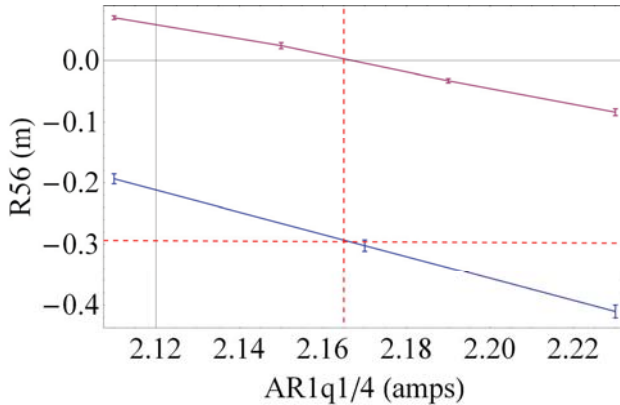


Figure 6: R_{56} vs. first arc quadrupole strength measured at the exit of the first arc (magenta) and the bunch compressor (blue). The red dotted line indicates the isochronous condition of the first arc.

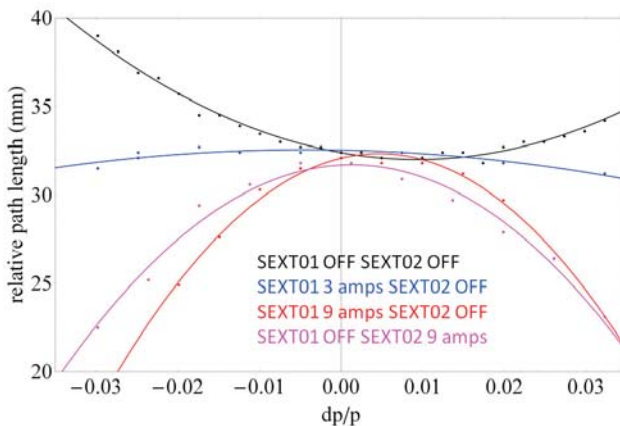


Figure 7: Relative path length vs. energy measured at the exit of the first arc for different arc sextupole (SEXT01 and SEXT02) strengths. Points are measurements, lines are parabolic fits.

CONCLUSION

The beam dynamics of the ALICE IR-FEL facility have been discussed, including longitudinal phase space measurement of the electron bunch, and recent measurements of the longitudinal transport functions of the lattice.

Direct measurements of the longitudinal bunch phase space have indicated bunch length and energy spread of the compressed bunch in agreement with the ALICE

design. However, the evolution of the bunch length and energy spread throughout the whole machine is not fully understood.

Longitudinal transport has been studied in the post-linac lattice by energy dependent path length measurements via bunch time of arrival measurements. These have confirmed and quantified the effect of the arc tuning on the longitudinal transport, in particular the post-linac R_{56} . The significant effect of the arc quadrupoles on the R_{56} has been measured quantitatively.

Finally the effect of the arc sextupoles on the path length vs. energy curvature (i.e. T_{566}) has been observed, and indications of R_{56} contribution via sextupole misalignment have been observed.

REFERENCES

- [1] M. W. Poole et al, '4GLS and the Energy Recovery Linac Prototype Project at Daresbury Laboratory', PAC '05, Tennessee.
- [2] Y. M. Saveliev, 'ALICE: Status, Developments and Scientific Programme', IPAC '12, New Orleans.
- [3] S. L. Smith et al, 'The Status of the Daresbury Energy Recovery Linac Prototype', PAC '07, Albuquerque.
- [4] S. Machida et al 'Acceleration in the linear non-scaling fixed-field alternating-gradient accelerator EMMA', Nature Physics 8, p243–247, (2012)
- [5] G. Priebe et al, "First results from the Daresbury Compton backscattering x-ray source (COBALD)", Proc. SPIE 7805, 780513 (2010).
- [6] N Thompson et al, 'First lasing of the ALICE infrared Free-Electron Laser', Nuclear Instruments and Methods A, Volume 680, 11 July 2012, Pages 117–123.
- [7] F. Jackson et al 'Beam Dynamics at the ALICE Accelerator R&D Facility', IPAC 2011, San Sebastian.
- [8] F. Jackson et al 'Longitudinal Beam Dynamics at the ALICE Accelerator R&D Facility', IPAC 2012, New Orleans.
- [9] Y. Saveliev et al 'Results from ALICE (ERLP) DC Photoinjector Gun Commissioning', EPAC '08, Genoa.
- [10] D. X. Wang et al 'Measurement of femtosecond electron bunches using a rf zero-phasing method', Phys. Rev. E 57, 2283–2286 (1998).
- [11] P. J. Phillips et al, 'Electro-Optic Bunch Diagnostics on ALICE', FEL 2009, Liverpool.
- [12] H. L. Owen et al "Choice of Arc Design for the ERL Prototype at Daresbury Laboratory", EPAC '04.